



Photoluminescence properties of $(\text{Ba}_{1-x}\text{Eu}_x)\text{WO}_4$ red synthesized by the coprecipitation/calcination method

Feng Wen-Lin^{a,c,*}, Zhao Ming-Fu^b, Xue Ji-Yuan^b, Tian Xiao-Jiao^a

^a Department of Applied Physics, Chongqing University of Technology, Chongqing 400054, China

^b Department of Electronic Information and Automation, Chongqing University of Technology, Chongqing 400054, China

^c International Centre for Materials Physics, Chinese Academy of Sciences, Shenyang 110016, China

ARTICLE INFO

Article history:

Received 30 October 2011

Received in revised form 11 January 2012

Accepted 16 January 2012

Available online 28 January 2012

Keywords:

Photoluminescence

Phosphor

Coprecipitation

$(\text{Ba}_{1-x}\text{Eu}_x)\text{WO}_4$

ABSTRACT

In this paper, we report on the series of novel red phosphors $(\text{Ba}_{1-x}\text{Eu}_x)\text{WO}_4$ were synthesized by coprecipitation/calcination method. The morphology and structure were characterized by scanning electron microscopy (SEM) and X-ray diffraction (XRD). Photoluminescence (PL) excitation and emission spectra were also used to characterize the $(\text{Ba}_{1-x}\text{Eu}_x)\text{WO}_4$. The results showed that all phosphors present a scheelite-type tetragonal structure with space group $(I4_1/a)$. The SEM images showed that the grains were like shuttles with sizes ranging from 3.0 to 7.0 μm . The obtained $(\text{Ba}_{1-x}\text{Eu}_x)\text{WO}_4$ phosphor emitted red emission centered at 612 nm corresponding to the ${}^5\text{D}_0 \rightarrow {}^7\text{F}_2$ transition of Eu^{3+} when was excited by 394 nm and 465 nm which well matched with near-ultraviolet and blue chips. The optimized concentration of Eu^{3+} was 20 mol.% for the highest PL emission intensity which was excited at 534 nm. The concentration quenching occurred when the Eu^{3+} concentration was beyond 20 mol.%.

© 2012 Elsevier B.V. All rights reserved.

1. Introduction

The growing interest in $\text{Eu}(\text{III})$ activated red phosphors is due to its high quantum efficiency, good stability and suitability for use in white light-emitting diodes (W-LEDs) [1–5]. However, the performance of the W-LEDs depends critically on the quality of tri-color phosphor stand or fall, which in turn depends on the host lattice. Among the tri-color phosphors, red phosphors have more significant effect on the luminous flux than green and blue. Eu^{3+} -doped materials show intense ${}^5\text{D}_0 \rightarrow {}^7\text{F}_2$ emission in the red spectral region, which have been diffusely adopted as red emitting phosphors [6]. Especially, the Eu^{3+} doped barium tungstate (BaWO_4) compounds may be a potential phosphor due to its excellent physical and chemical properties [7]. Several methods such as polyol method [8], mild hydrothermal method [9] have been used to prepared Eu^{3+} doped barium tungstate phosphors.

Therefore, in the present paper, we report on the synthesis of $(\text{Ba}_{1-x}\text{Eu}_x)\text{WO}_4$ phosphor by a coprecipitation/calcination method which can produce good morphology and chemical uniformity of the powders. The structure, PL excitation and emission spectra of the phosphors have been investigated in detail. The optimized

concentration and quenching mechanism of Eu^{3+} have also been discussed.

2. Experimental

2.1. Synthesis of $(\text{Ba}_{1-x}\text{Eu}_x)\text{WO}_4$

$(\text{Ba}_{1-x}\text{Eu}_x)\text{WO}_4$ ($0.1 \leq x \leq 0.4$) red phosphors were prepared by coprecipitation/calcination method. Eu_2O_3 (99.99%), $\text{BaCl}_2 \cdot 2\text{H}_2\text{O}$ (A.R.), $\text{Na}_2\text{WO}_4 \cdot 2\text{H}_2\text{O}$ (A.R.) and $\text{NH}_3 \cdot \text{H}_2\text{O}$ (A.R.) were used as the starting materials. Firstly, stoichiometric Eu_2O_3 was dissolved in diluted nitric acid (A.R., 80 mL). $\text{BaCl}_2 \cdot 2\text{H}_2\text{O}$ and $\text{Na}_2\text{WO}_4 \cdot 2\text{H}_2\text{O}$ were dissolved in deionized water (80 mL), then the solution was mixed under magnetic stirring, and form stock solution; the stock solution was dropped in ammonium hydroxide (80 mL) and then white precipitation was obtained. After aging, filtration, washing, and drying, the white precursor was obtained. The precursor was calcined at 900 °C for 2 h, and then the red phosphor $(\text{Ba}_{1-x}\text{Eu}_x)\text{WO}_4$ without milling was obtained.

2.2. Characterization

The XRD of $(\text{Ba}_{1-x}\text{Eu}_x)\text{WO}_4$ was carried out by XRD-6000-Shimadzu Scientific Instruments with $\text{Cu K}\alpha$ radiation ($\lambda = 0.15406 \text{ nm}$) at 40 kV and 30 mA. The morphology and structure of samples were measured by KYKY-1000B scanning electron microscope (SEM) and the scanning range and speed were 15° – 75° and $3^\circ/\text{min}$, respectively. PL excitation and emission spectra were observed by RF-5301 Molecular Fluorescence Spectrophotometer equipped with xenon lamp as excitation source. The excitation and emission slit was 3 nm. All the measurements were operated at room temperature.

* Corresponding author at: Department of Applied Physics, Chongqing University of Technology, Chongqing 400054, China. Tel.: +86 023 62563051.

E-mail address: wenlinfeng@126.com (W.-L. Feng).

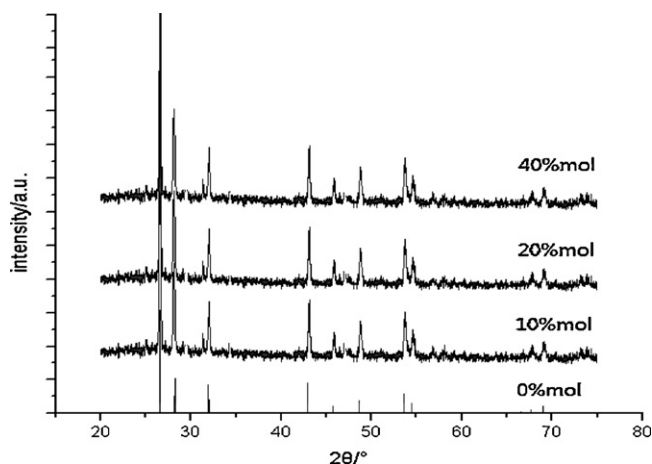


Fig. 1. XRD patterns of $(\text{Ba}_{1-x}\text{Eu}_x)\text{WO}_4$.

3. Results and discussion

3.1. The XRD analysis of sample

Fig. 1 shows diffraction peak of $(\text{Ba}_{1-x}\text{Eu}_x)\text{WO}_4$ sample with $x = 0, 0.1, 0.2, 0.4$ prepared by coprecipitation/calcination method. In this figure, XRD pattern revealed that all diffraction peaks of $(\text{Ba}_{1-x}\text{Eu}_x)\text{WO}_4$ powders can be indexed to the scheelite-type tetragonal structure with space group ($I4_1/a$) in agreement with the respective Joint Committee on Powder Diffraction Standards (JCPDS) card No. 72-0747. This result indicated that the replacement of Eu^{3+} could not change the crystal structure of the host. Considering the radius of Eu^{3+} (0.095 nm) smaller than that of Ba^{2+} (0.134 nm), but larger than that of W^{6+} (0.062 nm) [10], thus, Eu^{3+} ion should replace the Ba^{2+} site of BaWO_4 .

3.2. The morphological analysis of sample

The SEM images of $(\text{Ba}_{1-x}\text{Eu}_x)\text{WO}_4$ phosphor samples are presented in Fig. 2. It can be seen that $(\text{Ba}_{1-x}\text{Eu}_x)\text{WO}_4$ phosphor samples are made up of shuttle-shaped appearance distributed with diameters in the range of 3–7 μm . From the morphology of $(\text{Ba}_{1-x}\text{Eu}_x)\text{WO}_4$, the growth mechanism of $(\text{Ba}_{1-x}\text{Eu}_x)\text{WO}_4$ maybe like that of BaMoO_4 microcrystal [11,12], in the growth process, when two crystals are oriented in the same crystallographic direction and thus coalesce, the adhesion of two crystals can occur with the highest probability. The adhesion with the second highest probability usually occurs when two crystals has a “twin relation” (this case is known as “contact twin”). Moreover, when two crystals have

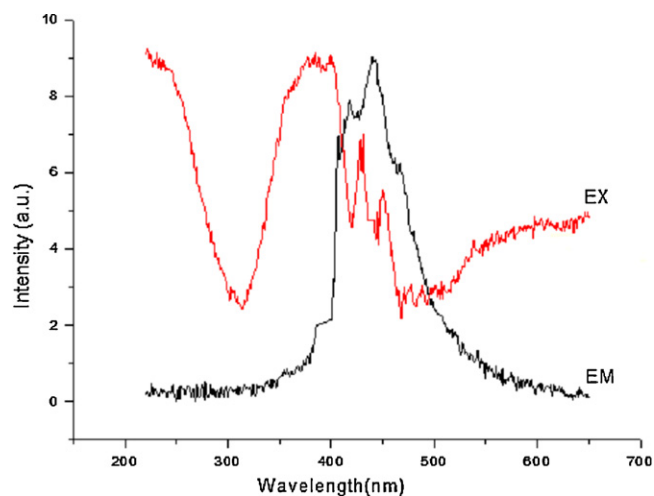


Fig. 3. Excitation and emission spectra of pure BaWO_4 .

some specific crystallographic relations, called “coincidence site lattice matching”, two crystals adhere strongly [11,12].

3.3. The PL excitation and emission analysis of $(\text{Ba}_{1-x}\text{Eu}_x)\text{WO}_4$

The excitation and emission spectra are, respectively, recorded by monitoring at 399 nm and 440 nm, as given in Fig. 3. For PL emission spectra of BaWO_4 pure crystal, during the excitation process at room temperature, the electrons situated at lower intermediary energy levels (oxygen 2p states) absorb the photon energies arising from different wavelengths. As consequence of this phenomenon, the energetic electrons are promoted to higher intermediary energy levels (tungsten 4d states) located near the conduction band. When the electrons fall back to lower energy states again via radiative return processes, the energies arising from this electronic transition are converted in photons [13]. In this case, the several photons originated by the participation of different energy states during the electronic transitions are responsible for the broad PL spectra (410–480 nm).

In Fig. 4, the PL excitation spectra are recorded by monitoring at 610 nm. Some narrow peaks of f–f transition absorption of Eu^{3+} ions are, respectively, ${}^7\text{F}_0 \rightarrow {}^5\text{L}_6$ (394 nm), ${}^7\text{F}_0 \rightarrow {}^5\text{D}_2$ (465 nm) and ${}^7\text{F}_0 \rightarrow {}^5\text{D}_1$ (534 nm). Thus, the red phosphor $(\text{Ba}_{1-x}\text{Eu}_x)\text{WO}_4$ has excellent absorption ability in near-UV, blue and green light, especially the near-UV and blue light have a good absorption, which can be excited by the commercial near-UV (394 nm) and blue LED chips (465 nm).

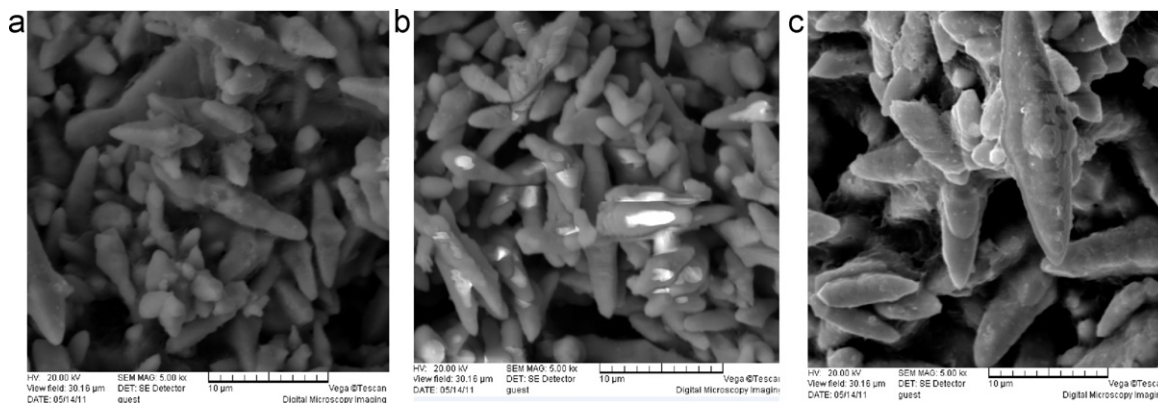


Fig. 2. SEM images of $(\text{Ba}_{1-x}\text{Eu}_x)\text{WO}_4$.

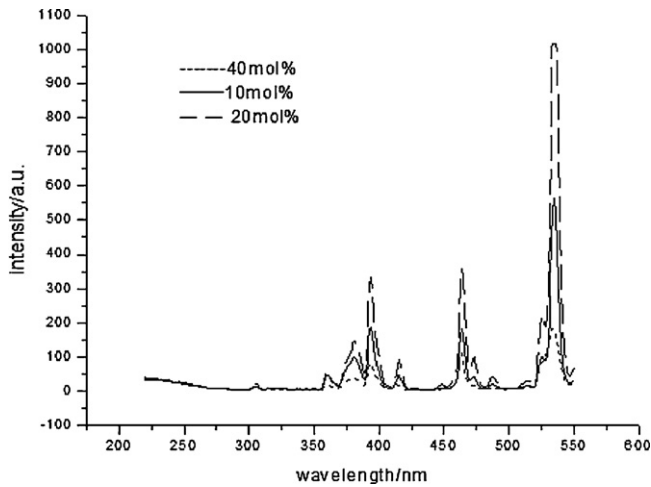


Fig. 4. Excitation spectra of the different doses doped $(\text{Ba}_{1-x}\text{Eu}_x)\text{WO}_4$, $\lambda_{em} = 610$ nm.

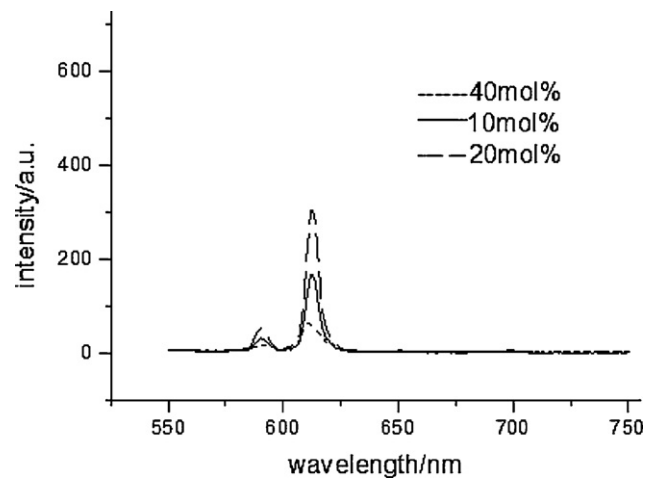


Fig. 5. Emission spectra of the different doses doped $(\text{Ba}_{1-x}\text{Eu}_x)\text{WO}_4$, $\lambda_{ex} = 394$ nm.

From Figs. 5–7, one can see that the emission spectrum of $(\text{Ba}_{1-x}\text{Eu}_x)\text{WO}_4$ ($x = 0.1, 0.2, 0.4$) excited by 394, 465 and 534 nm at room temperature, respectively, is composed of a series of sharp lines, which is similar to the emission of Eu^{3+} in other host crystals

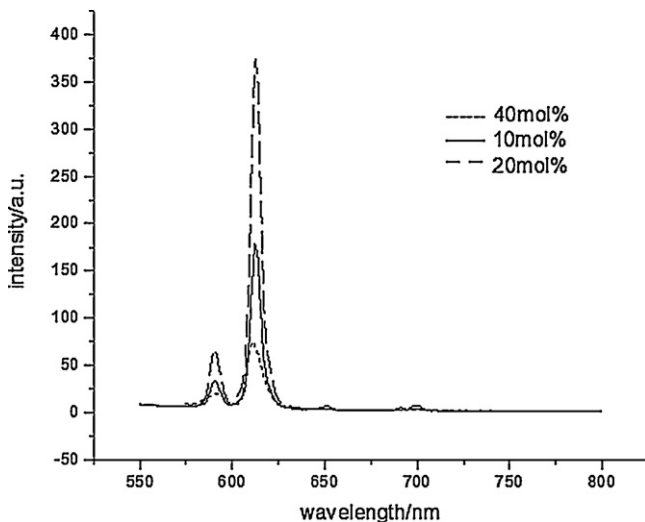


Fig. 6. Emission spectra of the different doses doped $(\text{Ba}_{1-x}\text{Eu}_x)\text{WO}_4$, $\lambda_{ex} = 465$ nm.

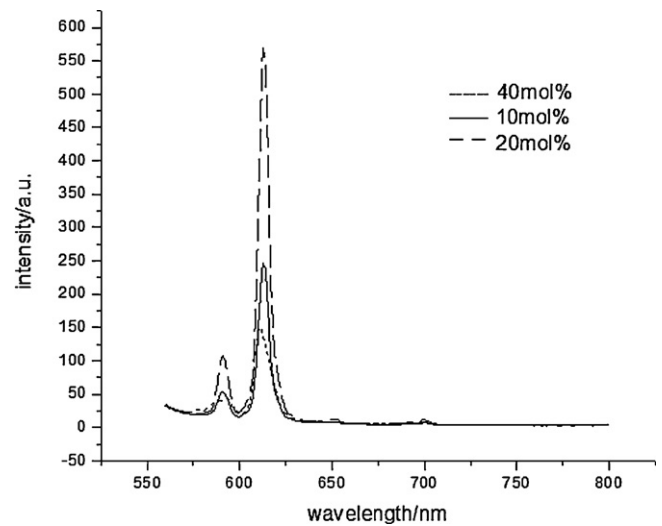


Fig. 7. Emission spectra of the different doses doped $(\text{Ba}_{1-x}\text{Eu}_x)\text{WO}_4$, $\lambda_{ex} = 534$ nm.

[14,15]. The strongest red emission is located at 612 nm attributing to electric dipole transition ${}^5\text{D}_0 \rightarrow {}^7\text{F}_2$ of Eu^{3+} ion, while the weak orange emission located around 590 nm is belonging to the magnetic dipole transition ${}^5\text{D}_0 \rightarrow {}^7\text{F}_1$. It also can be seen that transition intensity of ${}^5\text{D}_0 \rightarrow {}^7\text{F}_2$ increases first and decline with the increase of molar amount of doped Eu^{3+} , and transition intensity gets the maximum as doping fraction at 0.2. When the amount of Eu^{3+} is lower than 0.2, increasing the doping amount, which can increase luminance brightness; when the amount of Eu^{3+} is more than 0.2, increasing the doping amount will reduce the coherent dispersity of crystal lattice of the host and increase the probability of non-radiative process involving cross-relaxation [16], leading to the decline of luminescent efficiency and causing the concentration quenching.

4. Conclusion

In summary, $(\text{Ba}_{1-x}\text{Eu}_x)\text{WO}_4$ red phosphors have been synthesized by coprecipitation/calcination method. The investigated results indicate that the $(\text{Ba}_{1-x}\text{Eu}_x)\text{WO}_4$ phosphor is a promising red phosphor for both near-UV and blue based white LED. The growth and PL emission mechanism of $(\text{Ba}_{1-x}\text{Eu}_x)\text{WO}_4$ have been analysed in the present work. The concentration quenching mechanism can be explained by the dopant inducing the non-radiative mechanism.

Acknowledgements

Project supported by the National Science Foundation of China (Grant Nos. 11104366 and 50876120), the Natural Science Foundation Project of CQ (Grant No. CSTC2011jjA50015) and the Foundation of the Research Group for Universities of Chongqing (Grant No. 201023).

References

- [1] Y.L. Yang, X.M. Li, W.L. Feng, W.J. Yang, W.L. Li, C.Y. Tao, J. Alloys Compd. 509 (2011) 845.
- [2] C.G. Ma, M.G. Brik, V. Kiisk, T. Kangur, I. Sildos, J. Alloys Compd. 509 (2011) 3441.
- [3] Y.L. Yang, X.M. Li, W.L. Feng, W.L. Li, C.Y. Tao, J. Alloys Compd. 505 (2010) 239.
- [4] Z.Y. Zhang, Y.H. Wang, F. Zhang, H.N. Cao, J. Alloys Compd. 509 (2011) 5023.
- [5] C.T. Lee, F.S. Chen, C.H. Lu, J. Alloys Compd. 490 (2010) 407.
- [6] N. Dhananjaya, H. Nagabhushana, B.M. Nagabhushana, B. Rudraswamy, C. Shivakumara, R.P.S. Chakradhar, J. Alloys Compd. 509 (2011) 2368.
- [7] L.S. Cavalcante, J.C. Sczancoski, J.W.M. Espinosa, J.A. Varela, P.S. Pizani, E. Longo, J. Alloys Compd. 474 (2009) 195.

- [8] H.L. Li, Z.L. Wang, J.H. Hao, *IOP Conf. Ser. Mater. Sci. Eng.* 1 (2009) 012010.
- [9] J. Liao, B. Qiu, H.R. Wen, Y. Li, R.J. Hong, H.Y. You, *J. Mater. Sci.* 46 (2010) 1184.
- [10] R.C. Weast, *CRC Handbook of Chemistry and Physics*, CRC Press, Boca Raton, 1989, F-187.
- [11] L.S. Cavalcante, J.C. Sczancoski, R.L. Tranquilin, J.A. Varela, E. Longo, M.O. Orlandi, *Particuology* 7 (2009) 353.
- [12] L.S. Cavalcante, J.C. Sczancoski, L.F. Lima, J.W.M. Espinosa Jr., P.S. Pizani, J.A. Varela, E. Longo, *Cryst. Growth Des.* 9 (2009) 1002.
- [13] J.C. Sczancoski, L.S. Cavalcante, N.L. Marana, R.O. da Silva, R.L. Tranquilin, M.R. Joya, P.S. Pizani, J.A. Varela, J.R. Sambrano, M.S. Li, E. Longo, J. Andrés, *Curr. Appl. Phys.* 10 (2010) 614.
- [14] Md. Masuqul Haque, H.I. Lee, D.K. Kim, *J. Alloys Compd.* 481 (2009) 792.
- [15] S. Choi, Y.M. Moon, K. Kim, H.K. Jung, S. Nahm, *J. Lumin.* 129 (2009) 988.
- [16] M. Inokuti, F. Hirayama, *J. Chem. Phys.* 43 (1965) 1978.